Sensors and Materials, Vol. 34, No. # (2022) 1–##
MYU Tokyo

S & M ####

Development of Colorimetric DNA Sensing System for Methicillin-resistant *Staphylococcus aureus* without Bond/Free Separation by Size Separation of Gold Nanoparticle Conjugates Using 2,2,6,6-Tetramethylpiperidine 1-oxyl (TEMPO)-oxidized Cellulose Nanofiber Cross-linked Filters

Shunsuke Kezuka,[1] Haruna Nakayama,[1] Yuko Morita,[2] Hiroaki Sakamoto,[1*]
Takeo Kitamura,[2] Masayuki Hashimoto,[2] Eiichiro Takamura,[1] and Shin-ichiro Suye[1]

[1]Frontier Fiber Technology and Science, Graduate School of Engineering, University of Fukui,
Bunkyo 3-9-1, Fukui 910-8507, Japan
[2]DKS Co. Ltd., 5 Ogawara-cho, Kisshoin, Minami-ku, Kyoto 601-8391, Japan

(Received November 22, 2021; accepted February 24, 2022; online published April 4, 2022)

Keywords: TEMPO-oxidized cellulose nanofiber, AuNP, biosensor, MRSA, probe

In recent years, infectious diseases caused by drug-resistant bacteria have been expanding worldwide. Methicillin-resistant *Staphylococcus aureus* (MRSA) is a type of drug-resistant bacterium that causes nosocomial infections. To detect nosocomial infections at an early stage, it is important to develop a rapid and simple method to detect MRSA. In this study, we developed a simple colorimetric biosensor that separates target DNA-probe-modified gold nanoparticles (AuNPs) using a freeze-dried Ca^{2+}-cross-linked 2,2,6,6-tetramethylpiperidine 1-oxyl (TEMPO)-oxidized cellulose nanofiber (TOCN) filter. First, the AuNP probe was hybridized with the target ssDNA to form a complex. Because of the large size of the DNA–AuNP probe complex, it was trapped by the filter and showed the red color characteristic of AuNPs. The color intensity of the AuNPs increased with the DNA concentration. The color filter sensor was able to quantify the target DNA in the range of 10–1000 pM without polymerase chain reaction (PCR) amplification (3.0×10^8–3.0×10^{10} copies). The sensor we developed can filter out unreacted AuNP probes, thus eliminating the need for bond/free (B/F) separation. Our sensing system was able to finish detection in 1 min and was selective enough to distinguish between MRSA and *S. aureus* (SA).

1. Introduction

Methicillin-resistant *Staphylococcus aureus* (MRSA) is a bacterium that has acquired resistance to β-lactam antibiotics. It has been known to cause nosocomial infections since it was first reported in the United Kingdom in 1961.[(1–3)] MRSA is opportunistic and causes widespread infections in immunocompromised patients.[(4)] Delayed treatment can lead to fatal consequences,

*Corresponding author: e-mail: hi-saka@u-fukui.ac.jp
https://doi.org/10.18494/SAM3735

ISSN 0914-4935
https://myukk.org/

such as pneumonia, osteomyelitis, and sepsis.[5] Therefore, a rapid and simple method for detecting MRSA is needed to prevent the spread of infection and epidemic.

Conventional testing methods for MRSA include drug susceptibility testing.[6,7] In this method, the bacteria in the specimen collected from the patient are propagated by culture and confirmed by reaction to antibiotics. However, although the culture method has high detection sensitivity, it takes a long time before results are obtained; hence, rapid detection is not possible.

In recent years, nanoparticle-based biosensors have been actively studied as tools for detecting target DNA. Nanoparticles are modified with probes, and the target DNA is collected and quantified by various methods.[8–10] The behavior change of fluorescent particles can be captured by fluorescence microscopy using this property, and MRSA can be detected by image analysis.[11] Recently, bimodal waveguide interferometry and microchip electrophoresis have also been developed to detect MRSA.[12,13]

Previously, we developed a rapid and simple electrochemical biosensing system for MRSA using the molecular recognition function of DNA. Gold nanoparticles (AuNPs) are modified with a ferrocene derivative, which is responsible for electron transfer between the probe and the enzyme electrode, to form a complex with the target DNA. The oxidation current based on the oxidation of ferrocene is then measured to detect MRSA.[14]

We have also developed a fluorescence sensor using fluorescent particles. The AuNPs and fluorescent particles are modified with probes to form a complex with the target DNA. The larger the amount of the target DNA, the larger the size of the complex and the lower the diffusivity of the fluorescent particles.[15] Both methods can detect MRSA in a rapid and simple step; however, the disadvantage of these methods is the high cost of the potentiostat and fluorescence microscope, which are the detection parts, and there is a need to reduce the cost of materials for the detection parts.

In this study, we propose a rapid, simple, accurate, and low-cost method for the detection of MRSA using filters. We used a 2,2,6,6-tetramethylpiperidine 1-oxyl (TEMPO)-oxidized cellulose nanofiber (TOCN) filter, which is formed by chemically dissociating cellulose with a catalyst called TEMPO.[16–18] TOCN is a nanofiber of 4 nm diameter and is expected to be used for industrial applications. Freeze-dried TOCN produces an aerogel with a spiderweb-like network, which has been applied as a gas filter owing to its high specific surface area and excellent network structure.[19,20] However, by cross-linking TOCN with heavy metal ions, the wet strength was improved and a highly durable film was successfully fabricated.[21] In addition, by taking advantage of the three-dimensional network and high specific surface area of TOCN cross-linked aerogels, they have been applied to adsorbents suitable for water purification.[22] These results suggest that aerogels prepared using TOCN cross-linked membranes have the potential to develop new applications as filters for liquids. In addition, TOCN cross-linked membranes are more suitable for quantitative sensing materials than conventional paper filters because the pore size and thickness can be controlled and prepared by changing the drying and cross-linking methods. Therefore, we fabricated a TOCN-based sensor filter and used it as the detection part of a DNA sensor. We modified AuNPs with probes and hybridized target single-stranded DNA (ssDNA) to form a complex. The probe sequence is complementary to a portion of the *mecA* region of MRSA. The size of the complex is expected to increase with the amount of

ssDNA. Therefore, when the complex is dropped onto the filter, if more target DNA is present, more of the complex will be trapped by the filter (Fig. 1). Because the trapped complex has a color tone unique to AuNPs, it is possible to visually confirm the presence of bacteria. We quantified the target DNA by comparing the color of the AuNPs on the filter. Conventional sensors need to remove unreacted particles (B/F separation) to increase the detection sensitivity. For this purpose, magnetic separation or centrifugation is necessary, but these methods are cumbersome. However, the sensor we developed performs detection and separation functions simultaneously, eliminating the need for B/F separation and enabling rapid detection. Paper-based biosensors are simple, inexpensive, and disposable, but they are affected by the diffusion of the fluid and lack quantitative performance.[23,24] The sensor we developed, however, uses suction filtration with a constant force to suppress the horizontal diffusion of the fluid, thereby eliminating the effect of diffusion. In addition, the filtering experiment can be completed in approximately 1 min. The image obtained can be analyzed and quantified using a computer; therefore, dedicated analysis equipment is not required. In this study, we developed a low-cost, disposable, and rapid DNA sensor without polymerase chain reaction (PCR) amplification.

2. Materials and Methods

2.1 Materials

AuNPs with an average diameter of 40 nm were purchased from BBI Solutions (Wiltshire, UK). Dried yeast extract, tryptone, and sodium chloride were purchased from Nacalai Tesque (Kyoto, Japan). EDTA・2Na, 2-amino-2-hydroxymethyl-1,3-propanediol, and hydrochloric acid were purchased from Wako Pure Chemical Industries (Osaka, Japan). All other chemicals were of analytical grade. TOCN was provided by DKS Co., Ltd.

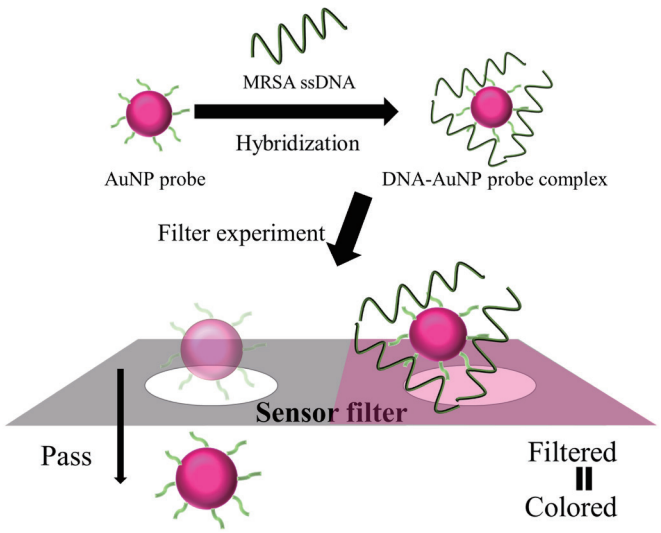

Fig. 1. (Color online) Mechanism of colorimetric filter sensor.

Deionized water filtered through a Milli-Q water purification system (Millipore Co., Bedford, MA, USA) was used for the experiments in this study. The filter holder was a Swinney filter holder (13 mm, stainless steel; Millipore), and RHEOCRYSTA I-2SX (DKS Co., Ltd.) was used.

2.2 Procedure

2.2.1 Preparation of sensor filter

A TOCN solution (5 ml, 0.4 wt%) was sonicated and stirred for 1 h. A calcium chloride solution (750 µl, 0.2 g/ml) was added to the TOCN solution and stirred to obtain a TOCN-Ca^{2+} solution. The TOCN-Ca^{2+} solution was frozen at −0 °C for 3 h and then lyophilized to prepare the sensor filter [Fig. 2(a)].

2.2.2 Sensor filter observation using FE-SEM

The prepared sensor filter was collected with tweezers to a size of 1 × 1 mm^2 and fixed on a silicon wafer. The fixed sample was coated with an osmium coater (HPC-1SW, vacuum device current: 10 mA, time: 10 s) and observed using FE-SEM (ULTRA plus, ZEISS: magnification: 10000×, acceleration voltage: 5000 V). The pore size of the sensor filter was measured from the FE-SEM images using ImageJ, and the pore size distribution was calculated.

2.2.3 Design of DNA probe

DNA probes targeting the MRSA *mecA* gene were purchased from Hokkaido System Science Corporation (Hokkaido, Japan). The sequence of the DNA probe used in this study is as follows: Probe 5′-TCTGGAACTTGTTGAGCAGAGGTTC-3′. A thiol group was introduced at the 5′ end of the probe in order to bind to AuNPs. Probes were dissolved in TE buffer and stored at 4 °C.

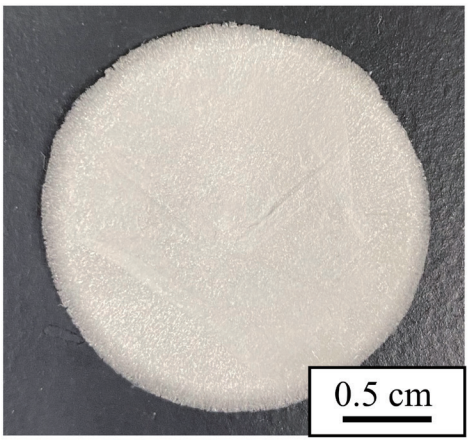

Fig. 2. (Color online) Sensor filter.

Tris-EDTA (TE) buffer was prepared by mixing 2-amino-2-hydroxymethyl-1, 3-propanediol and EDTA•2Na to final concentrations of 10 and 1 mM, respectively, and pH 8.0 by adding NaOH.

2.2.4 Preparation of AuNP probe

The AuNP probe was prepared by adding 0.1 nmol of probe to 50 µl of AuNPs with a particle count of 5×10^{12} particles/ml and allowing it to stand overnight at 4 °C (Fig. 3).

2.2.5 Preparation of DNA–AuNP probe complex

MRSA was obtained from the American Type Culture Collection (Manassas, VA, USA) and cultured overnight at 37 °C in Luria-Bertani (LB) medium. The genomic DNA of MRSA was extracted using TAKARA's® AXG Column NucleoBond® Buffer Set III (Shiga, Japan). The extracted dsDNA was stored in a TE buffer (pH 8.0) and used for subsequent experiments. The dsDNA solution was dissociated into ssDNA by heat treatment at 95 °C for 10 min. The ssDNA was added to the AuNP probe and hybridized at 45 °C for 45 min to produce DNA–AuNP probe complexes (Fig. 3).

2.2.6 Measurement of particle size of DNA–AuNP probe complex by dynamic light scattering (DLS) method

A nanoparticle analyzer (SZ-100V2) was used to observe the particle size of the DNA–AuNP probe complexes. The DNA–AuNP probe complexes (100 µl) were scaled up to 1 ml using a TE buffer and used as DLS samples. The particle size of the prepared sample was measured by the DLS method (temperature: 25 °C).

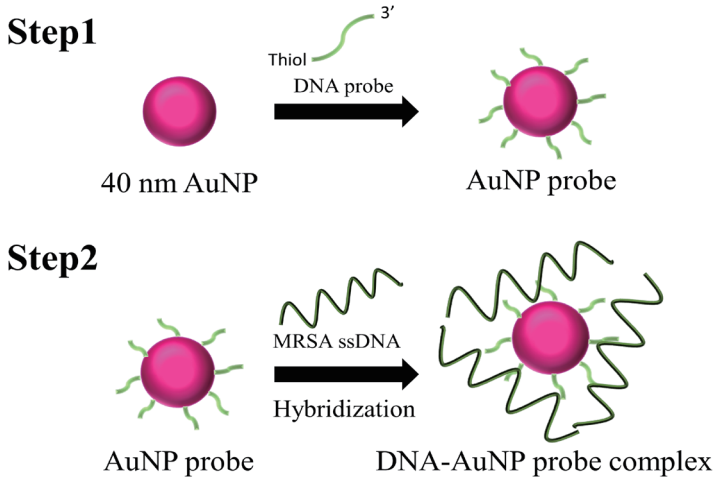

Fig. 3. (Color online) Preparation of DNA–AuNP probe complex. In step 1, AuNPs and probe were combined by Au–S bonding. In step 2, the AuNP probe and MRSA ssDNA were combined.

2.2.7 Sensor experiment

The sensor filter was cut into a circle of less than 1 cm diameter and sandwiched between two filter holders. We dropped 100 µl of DNA–AuNP probe complexes prepared at genomic DNA (MRSA) concentrations of 0, 1, 10, 100, and 1000 pM onto the filter holders, and suction filtration was performed at 36 L/min for 1 min. The color intensity of the color images obtained by suction filtration was calculated using ImageJ. The shading of the sensor filter can be expressed as a number from 0 to 255 using the histogram function of ImageJ, where black is 0 and white is 255. This function was used to quantify the shading of the DNA–AuNP probe complex on the sensor filter.

3. Results and Discussion

3.1 Analysis of sensor filter using FE-SEM

An FE-SEM image of the surface of the sensor filter is shown in Fig. 4(a). The sensor filter was porous, and a network was formed. The pore size of the sensor filter was measured using ImageJ. A histogram of the calculated pore size distribution is shown in Fig. 4(b). The results

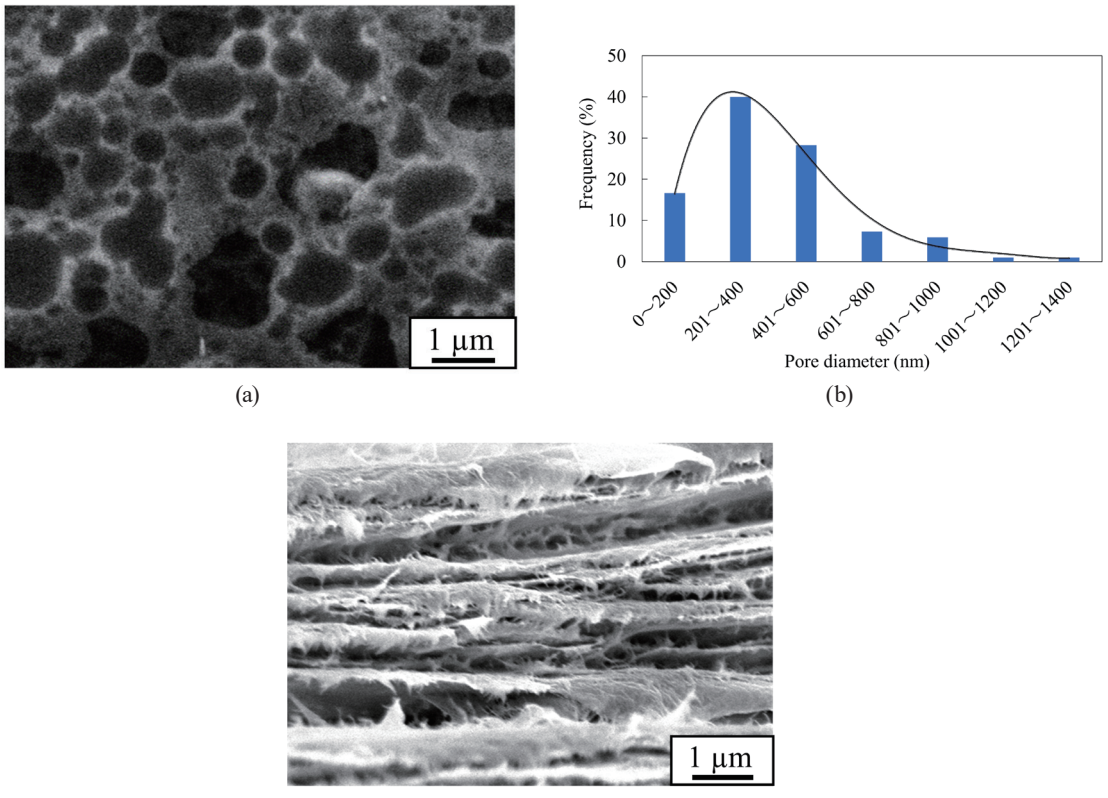

(a) (b)

(c)

Fig. 4. (Color online) (a) FE-SEM image of the pores of the sensor filter. (b) Pore size distribution of sensor filters measured using ImageJ. (c) FE-SEM image of the layered structure of a sensor filter.

show that the sensor filter retained pores of 0–1.4 μm size. The pore size of 200–400 nm was the most widely distributed. This non-uniform pore size originated from the ice crystals purified by pre-freezing. Therefore, the pore size can be adjusted by varying the water content of the frozen solution and the freezing temperature. A cross-sectional image of the film is shown in Fig. 4(c). It was confirmed that the self-assembly of TOCN resulted in the formation of a sheet-like multilayer structure. These results suggest that the sensor filter is suitable for the size-based separation of materials because the object can be supplemented not only on the surface of the film, but also inside.

3.2 Measurement of particle size of DNA–AuNP probe complexes using DLS

The particle size of the DNA–AuNP probe complex is shown in Fig. 5, and the major peaks are shown in Fig. 6. The diameter of the AuNP was 39.68 nm, confirming that the AuNPs were

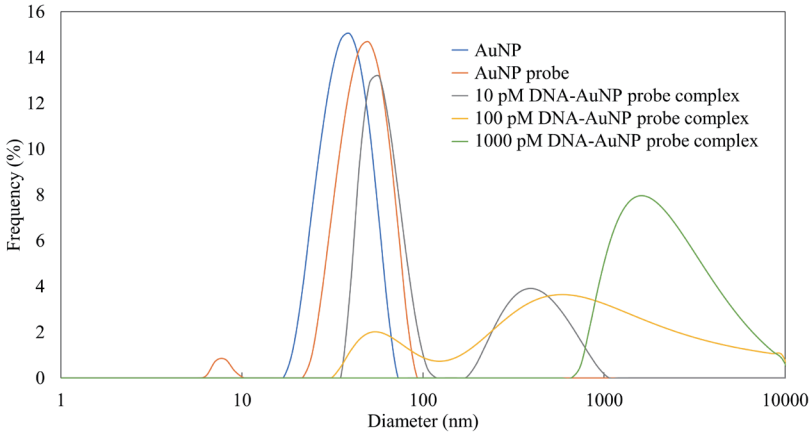

Fig. 5. (Color online) Measurement of particle size of DNA–AuNP probe complexes using DLS.

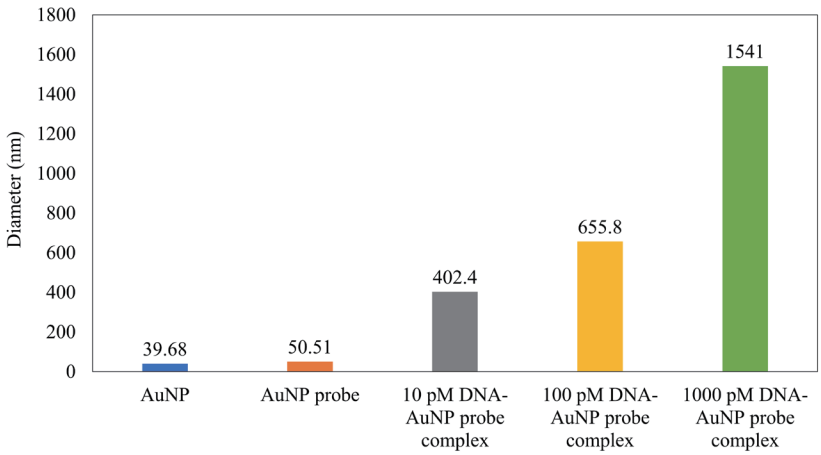

Fig. 6. (Color online) Major peaks obtained from DLS measurements (Fig. 5).

well dispersed. The AuNP probe showed two peaks at around 10 and 50.51 nm. The peak around 10 nm is considered to be from the unreacted probe, whereas the peak at 50.51 nm suggests that the probe is modified on the AuNP surface by Au–S bonds. Two peaks were observed for the DNA–AuNP probe complex at 10 and 100 pM. For DNA concentrations of 10 and 100 pM, the peaks at about 402.4 and 655.8 nm were observed, respectively. This suggests that the AuNP probe hybridized with the target DNA. A 1000 pM DNA–AuNP probe complex showed a single peak at around 1541 nm, indicating complete hybridization between the AuNP probe and the target DNA.

3.3 Detection of MRSA using a sensor filter and selectivity evaluation

Figure 7 shows the color images of the DNA–AuNP probe complexes prepared with 1, 10, 100, and 1000 pM MRSA and SA DNA dropped onto the sensor filter and separated. We first focus on the image when MRSA DNA is used. In Fig. 7, it was confirmed that the color of the AuNPs became darker as the DNA concentration increased. The color intensity of AuNPs was then calculated and the results are shown in Fig. 8. The gray scales of the color intensity of the complexes at concentrations of 0, 1, 10, 100, and 1000 pM DNA (MRSA) were 1.46, 6.9, 18.5, 71.3, and 109.7, respectively. The color intensity of AuNPs correlated with the concentration of DNA and increased exponentially. This suggests that DNA binds to the AuNP probe, increasing the size and number of the complex. The color of the AuNPs was red in solution, but became purple when dropped onto the sensor filter. Therefore, the sensor filter after the separation of the DNA–AuNP probe complex was observed by FE-SEM (Fig. 9). The change in the color of the AuNPs from red to purple was due to the formation of these aggregates. This is because the DNA–AuNP probe complexes were added to the fine pores of the sensor filter, promoting aggregation.[25] In addition, suction filtration was used to reduce the lateral spread of the liquid.

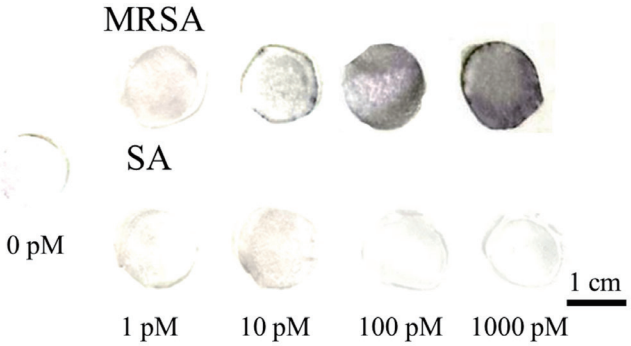

Fig. 7. (Color online) Photographs of TOCN cross-linked sensor membrane filter surface after separation of hybridization complex of probe-modified AuNPs and MRSA DNA.

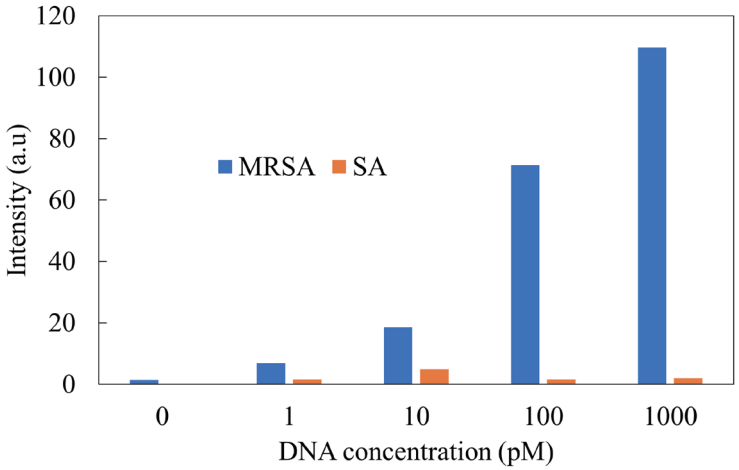

Fig. 8. (Color online) Profiles of color intensities of MRSA or SA DNA–AuNP probe complexes on sensor filter, calculated using the histogram function of ImageJ.

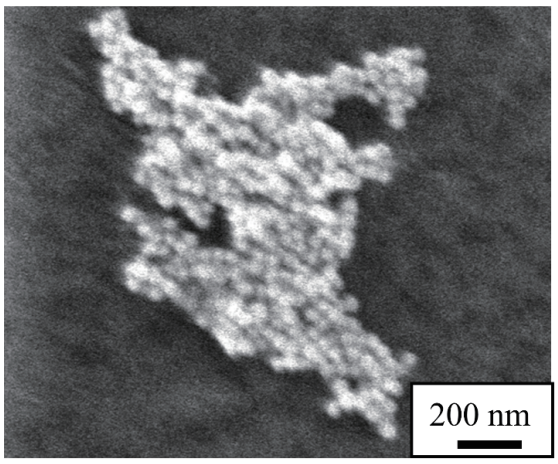

Fig. 9. Aggregates of 100 pM DNA–AuNP probe complex on sensor filter observed by FE-SEM.

Next, we focus on the image when SA is used. From the images, it was confirmed that the color of the AuNPs became lighter at all DNA concentrations when SA DNA was used. From Fig. 6, the gray scales of the color intensity of the complex at DNA (SA) concentrations of 1, 10, 100, and 1000 pM were 1.6, 4.9, 1.6, and 2.0, respectively. The color intensity did not correlate with the DNA concentration. In addition, Fig. 7 shows that the color intensity of MRSA was higher than that of SA at each concentration. In this study, we used a probe that binds specifically to MRSA DNA, and hence, does not bind to the DNA of other bacterial species and does not form a complex. Therefore, when a mixed solution of the AuNP probe and SA DNA was dropped onto the sensor filter, we considered that the AuNP probe passed through and the color intensity became low. These results indicate that the sensor can selectively recognize and detect the target DNA, because the coloration was different compared with when a different type of DNA was used.

4. Conclusion

In this study, we constructed a rapid, simple, and selective DNA sensing system using TOCN filters and AuNP probes. Genomic DNA from MRSA was recovered using AuNP probes. The sensor filter was prepared by cross-linking TOCN with calcium ions and freeze-drying. When the fabricated sensor filter was observed by FE-SEM, it was found to be porous, with many pores ranging from 200 to 400 nm. In addition, the formation of a layered structure was confirmed by the self-assembly of TOCNs. Next, the particle sizes of the DNA–AuNP probe complexes were measured using DLS. The DNA–AuNP probe complexes were found to be larger than the AuNP probe by hybridization with the target DNA. Next, the genomic DNA of MRSA was detected using the DNA-AuNP probe complex and the sensor filter. The DNA–AuNP probe complex was dropped onto a sensor filter and separated using a suction filtration system. The separation experiment using the filter was quick and easy, as it took only approximately 1 min to complete. The color intensity of the AuNPs showed a linear correlation with genomic DNA in the range of 10–1000 pM (3.0×10^8–3.0×10^{10} copies). This DNA sensing system using AuNP probes and sensor filters can detect the 10 pM genomic DNA of MRSA without PCR amplification. However, the practical application of the sensor developed in this study is still difficult because detection at 1 fM is actually required. Therefore, it is necessary to study the uniformity of the pore size of the filter and to optimize the dispersion of the AuNPs in the future. The selectivity experiment using the genomic DNA of SA, which does not contain the *mecA* region, the recognition sequence of the probe, resulted in low color intensity. This suggests that our color filter sensor can selectively recognize and detect the target DNA. Further studies are needed to demonstrate the sensor performance in bacterial lysate, where other proteins and nucleic acids are present.

The color filter sensor does not require B/F separation because the TOCN filter can separate the unreacted AuNP probes generated during hybridization formation. Therefore, no centrifugation or magnetic separation is required for separation, and the analysis can be performed at the patient's bedside or at other sites. In addition, the sensor filter is environmentally friendly and disposable because it is derived from cellulose. The TOCN filter-based colorimetric biosensor proposed in this study will be extremely useful for the early detection of MRSA because of its low cost, rapidity, and on-site detection.

References

1 M. Kuroda, T. Ohta, I. Uchiyama T. Baba H. Yuzawa I. Kobayashi, L. Cui, A. Oguchi, K. Aoki, Y. Nagai, J. Lian, T. Ito M. Kanamori, H. Matsumaru, A. Maruyama, H. Murakami, A. Hosoyama, Y.Mizutani-Ui, N. K. Takahashi, T. Sawano, R. Inoue, C. Kaito, K. Sekimizu, H. Hirakawa, S. Kuhara, S. Goto, J. Yabuzaki, M. Kanehisa, A. Yamashita, K. Oshima, K. Furuya, C. Yoshino, T. Shiba, M. Hattori, N. Ogasawara, H. Hayashi, and K. Hiramatsu: Lancet **357** (2001) 9264. https://doi.org/10.1016/S0140-6736(00)04403-2

2 G. Taubes: Science **321** (2008) 5887. https://doi.org/10.1126/science.321.5887.356

3 J. P. Addicks, S. Uibel, A. M. Jensen, M. Bundschuh, D. Klingelhoefer, and D. A. Groneberg: Int. J. Environ. Res. Public Health **11** (2014) 10. https://doi.org/10.3390/ijerph111010215

4 D. K. Corrigan, H. Schulze, G. Henihan, I. Ciani, G. Giraud, J. G. Terry, A. J. Walton, R. Pethig, P. Ghazal, J. Crain, C. J. Campbell, A. R. Mount, and T. T. Bachmann: Biosens. Bioelectron. **34** (2012) 1. https://doi.org/10.1016/j.bios.2012.01.040

5 F. C. Henry and R. D. Frank: Nat. Rev. Microbiol. **7** (2009) 629. https://doi.org/10.1038/nrmicro2200
6 E. Bessède, A. Delcamp, E. Sifrè, A. Buissonnière, and F. Mègraud: J. Clin. Microbiol. **49** (2011) 3. https://doi.org/10.1128/JCM.01489-10
7 L. Conza, S. Casati, and V. Gaia: BMC Microbiol. **13** (2013) 49. https://doi.org/10.1186/1471-2180-13-49
8 J. M. C. C. Guzman, S. M. Hsu, and H. S. Chuang: Biosensors **10** (2020) 10. https://doi.org/10.3390/bios10100130
9 T. A. Taton, C. A. Mirkin, and R. L. Letsinger: Science **289** (2000) 5485. https://doi.org/10.1126/science.289.5485.1757
10 O. Linda, R. Tomas, P. Indriati, K. Mikael, and H. Fredrik: Langmuir **19** (2003) 24. https://doi.org/10.1021/la0352927
11 K. Guk, J. O, Keem, S. G. Hwang, H. Kim, T. Kang, E. K. Lim, and J. Jung: Biosens. Bioelectron. **95** (2017) 67. https://doi.org/10.1016/j.bios.2017.04.016
12 J. aldonado, M. C. Estévez, A. Fernández-Gavela, J. J. González-López, A. B. González-Guerrero, and L. M. Lechuga: Analyst **145** (2020) 2. https://doi.org/10.1039/C9AN01485C
13 Y. Lu, F. Luo, Z. Li, G. Dai, Z. Chu, J. Zhang, F. Zhang, Q. Wang, and P. He: Talanta **222** (2021) 121686. https://doi.org/10.1016/j.talanta.2020.121686
14 K. Watanabe, N. Kuwata, H. Sakamoto, Y. Amano, T. Satomura, and S. Suye: Biosens. Bioelectron. **67** (2015) 419. https://doi.org/10.1016/j.bios.2014.08.075
15 J. C. Wang, Y. C. Tung, K. Ichiki, H. Sakamoto, T. H. Yang, S. Suye, and H. S. Chuang: Biosens. Bioelectron. **148** (2020) 111817. https://doi.org/10.1016/j.bios.2019.111817
16 A. Isogai and Y. Kato: Cellulose **5** (1998) 153. https://doi.org/10.1023/A:1009208603673
17 T. Saito, S. Kimura, Y. Nishiyama, and A. Isogai: Biomacromolecules **7** (2006) 6. https://doi.org/10.1021/bm060154s
18 A. Isogai, T. Hänninen, S. Fujisawa, and T. Saito: Prog. Polym. Sci. **86** (2018) 122. https://doi.org/10.1016/j.progpolymsci.2018.07.007
19 J. Nemoto, T. Soyama, T. Saito, and A. Isogai: Biomacromolecules **13** (2012) 3. https://doi.org/10.1021/bm300041k
20 J. Nemoto, T. Saito, and A. Isogai: ACS Appl. Mater. Interfaces **7** (2015) 35. https://doi.org/10.1021/acsami.5b05841
21 M. Shimizu, T. Saito, and A. Isogai: J. Membr. Sci. **500** (2016) 1. https://doi.org/10.1016/j.memsci.2015.11.002
22 X. Zhang, I. Elsayed, C. Navarathna, G. T. Schueneman, and E. B. Hassan: ACS Appl. Mater. Interfaces **11** (2019) 50. https://doi.org/10.1021/acsami.9b15139
23 H. Ki, H. Jang, J. Oh, G. R. Han, H. Lee, S. Kim, and M. G. Kim: Anal. Chem. **92** (2020) 17. https://pubs.acs.org/doi/10.1021/acs.analchem.0c02940
24 J. C. Cunningham, M. R. Kogan, Y. J. Tsai, L. Luo, I. Richards, and R. M. Crooks: ACS Sens. **1** (2016) 1. https://pubs.acs.org/doi/10.1021/acssensors.5b00051
25 H. N. Ying, L. Dan, P. S. George, and G. Gil: Langmuir **28** (2012) 23. https://doi.org/10.1021/la3012734